Frequency domain accuracy of approximate sampled-data models

Eduardo A. Yucra and Juan I. Yuz*

October 21, 2010

Abstract

Accurate sampled-data models are required when a digital device interacts with a continuous-time system. Even though exact sampled models can be obtained for linear systems, simple approximate models are sometimes preferred in applications to reduce computational load or to preserve the role of physical parameters. In this paper we quantify the frequency domain relative error of three kinds of approximate sampled models: (i) simple models obtained by derivative approximations (such as Euler and Tustin), (ii) models obtained including the asymptotic sampling zeros, and (iii) models obtained by a truncated Taylor expansion of the system state equations. In particular, we characterize the bandwidth where each of the proposed models provides the highest accuracy.

1 Introduction

Most real systems and processes evolve in continuous-time, however, nowadays most control strategies are implemented using digital devices. As a consequence, discrete-time representations are required to be, both, simple and accurate in order to achieve good performance of control strategies or in identification algorithms. For linear systems, exact sampled-data models can be obtained, for example, assuming a zero-order hold (ZOH) input (see, e.g., [4]). One of the consequences of the sampling process is the presence of, so called, *sampling zeros* in the associated discrete-time transfer function. These zeros have no counterpart in the underlying continuous-time model [3]. In fact, the specific characterization of these zeros depends on the hold device used to generate the input [12, 24, 2]. Similar results have been obtained for sampled models for linear stochastic systems [19, 21]. Moreover, in the nonlinear case, the presence of *sampling zero dynamics* has been also characterized based on normal forms [16, 15, 22, 11, 23, 13, 10].

In this paper we quantify the accuracy of approximate sampled-data models for linear deterministic systems in terms of the associated relative error in the frequency domain. Model accuracy is a key issue for control. In fact, there are cases where a controller based on an approximate model that stabilizes the nominal control loop for every sampling period $\Delta > 0$, may fail to stabilize the true continuous-time model no matter how small the sampling period is chosen [17]. In [6] the accuracy of a class of approximate sampled models (not considered in this paper) was characterized in terms of the ratio between the models as a function of the sampling period.

The current paper is a continuation of the work presented in [9] and [1] where approximate sampled models were considered for deterministic and stochastic systems, respectively. In particular, we extend the results in [9] by characterizing the bandwidth where the different models provide the highest accuracy. We include in the analysis a class of models obtained truncating the Taylor series expansion of the state equations (as in [22]) not been previously considered in [9].

The paper structure is as follows: Section 2 presents background on sampling of linear systems. Section 3 presents the approximate sampled-data models considered in the current work. In Section 4 we define the relative error measures and we obtain their $\mathcal{H}_\infty$ norm. The main results of the paper are presented in Section 5, where we study the bandwidth where each model provides the highest accuracy. Finally, Section 6 presents examples and Section 7 presents conclusions.

*Department of Electronic Engineering, Universidad Técnica Federico Santa María, Valparaíso, Chile. Email: eyucra@elo.utfsm.cl, juan.yuz@usm.cl

2 Background on sampling of linear systems

We consider a linear system given by the transfer function:

$$G(s) = \frac{F(s)}{E(s)} = \frac{\prod_{k=1}^{m}(s-\sigma_k)}{\prod_{i=1}^{n}(s-p_i)} \tag{1}$$

The system relative degree is $r = n - m > 0$. Note that if a gain is included in the model, it would only act as a scaling factor in our developments. We assume that the system input is generated using a zero-order hold (ZOH):

$$u(t) = u(k\Delta) = u_k \quad ; k\Delta \leq t < (k+1)\Delta \tag{2}$$

where Δ is the sampling period. If the system output is sampled instantaneously $y_k = y(k\Delta)$, then the exact sampled-data model is given by

$$G_d(z) = \frac{F_d(z)}{E_d(z)} = \frac{(z-1)}{z}\mathcal{Z}\left\{\mathcal{L}^{-1}\left\{\frac{G(s)}{s}\right\}\Big|_{t=k\Delta}\right\} \tag{3}$$

$$= \frac{(z-1)}{z}\frac{1}{2\pi j}\int_{\gamma-j\infty}^{\gamma+j\infty}\frac{e^{s\Delta}}{z-e^{s\Delta}}\frac{G(s)}{s}ds \tag{4}$$

where $\gamma > \max_i\{\mathfrak{Re}\{p_i\}\}$ and $\{p_i\}$ are the poles of $G(s)$. The complex integral in (4) can be solved closing the integration path to the left half of the complex plane [8], which leads to

$$G_d(z) = \frac{(z-1)}{z}\sum_{\ell=1}^{n+1}\text{Res}_{s=d_\ell}\left\{\frac{G(s)}{s}\frac{e^{s\Delta}}{z-e^{s\Delta}}\right\} \tag{5}$$

where $d_\ell \in \{0, p_1, \ldots, p_n\}$. Alternatively, if we close the integration path in (4) to the right half of the complex plane, we obtain [4]:

$$G_d(e^{s\Delta}) = (1-e^{-s\Delta})\sum_{\ell=-\infty}^{\infty}\frac{G(s+2\pi j\ell/\Delta)}{s\Delta+2\pi j\ell} \tag{6}$$

Equations (5) and (6) provide different insights about the sampled-data model: if we replace $s = j\omega$ in (6) we can notice the *aliasing* effect, i.e., the sampled-data frequency response is obtained by folding the continuous system frequency response down to the band $[-\frac{\pi}{\Delta}, \frac{\pi}{\Delta}]$. On the other hand, equation (5) shows a clear mapping of the systems poles from the continuous to the discrete domain, i.e., $s = p_i$ maps to $z = e^{p_i\Delta}$.

The mapping of the system zeros is much more involved. Moreover, the sampled-data model (3) has, in general, relative degree one. This means that there are *sampling zeros* in the discrete model which have no continuous-time counterpart. These extra zeros can be asymptotically characterized for fast sampling rates [3]:

$$G_d(z) \xrightarrow{\Delta\approx 0} \frac{\Delta^r\, B_r(z)\,(z-1)^m}{r!\,(z-1)^n} \tag{7}$$

where $B_r(z)$ are the Euler-Fröbenius polynomials [20].

$$B_r(z) = b_1^r z^{r-1} + b_2^r z^{r-2} + \ldots + b_r^r \tag{8}$$

$$b_k^r = \sum_{\ell=1}^{k}(-1)^{k-\ell}\,\ell^r\binom{r+1}{k-\ell} \tag{9}$$

These polynomials satisfy several properties:

1. From (8) and (9) it follows that $B_r(1) = r!$
2. The coefficients can be computed recursively, i.e., $b_1^r = b_r^r = 1$, for all $r \geq 1$, and
$$b_k^r = k b_k^{r-1} + (r-k+1)b_{k-1}^{r-1} \tag{10}$$
for $k = 2, \ldots, r-1$.
3. The coefficient are symmetric, i.e., $b_k^r = b_{r-k+1}^r$.It follows that
$$B_r(z) = z^{r-1}B_r(z^{-1}) \tag{11}$$
4. A consequence is that, when r is an even number, $B_r(-1) = 0$.
5. Their roots are always negative real and satisfy an interlacing property: every root of the polynomial $B_{r+1}(z)$ lies between every two adjacent roots of $B_r(z)$, for all $r \geq 2$.
6. The following recursive relation holds:
$$B_{r+1}(z) = z(1-z)B_r{}'(z) + (rz+1)B_r(z) \tag{12}$$
for all $r \geq 1$, and where $B_r{}' = \frac{dB_r}{dz}$.

Additionally, we will use the following property:

Lemma 1. *Let $B_r(z)$ be the polynomial of Euler-Fröbenius of order r, then the derivative at $z = 1$ is given by:*

$$B_r'(1) = \frac{r!(r-1)}{2} \tag{13}$$

Proof. If we differentiate equation (11) we obtain:

$$B_r'(z) = (r-1)z^{r-2}B_r(z^{-1}) - z^{r-3}B_r'(z^{-1}) \quad (14)$$

The result is obtained evaluating $z = 1$ and using property (1). □

3 Approximate sampled-data models

In this section we present the different approximate sampled models considered in our analysis. In the next sections we will compare the relative error associated with these models and their bandwidth of accuracy. We compare the proposed models with the **Exact Sampled Data** (ESD) model given in (3), i.e.,

$$G_d^{ESD}(z) = G_d(z) \quad (15)$$

We consider the following three classes of approximate sampled-data models

1. A **Simple Derivate Replacement** (SDR) model obtained using the Euler approximation for time derivatives, i.e., we replace $s = \frac{z-1}{\Delta}$ in (1):

$$G_d^{SDR}(z) = G(\tfrac{z-1}{\Delta}) \quad (16)$$

   This model does not include any sampling zero and has the same relative degree as the continuous-time system. In fact, this introduces additional delays in the sampled model (see, e.g., [18]).

   Additionally, we consider a **Tustin Derivate Replacement** (TDR) model, commonly used in applications. This model is based on a first order approximation of the natural logarithm $s = \ln(z)/\Delta$, i.e.

$$G_d^{TDR}(z) = G\big(\tfrac{2}{\Delta}\tfrac{z-1}{z+1}\big) \quad (17)$$

   This model has relative degree equal to 0, but does not include any of the sampling zeros in (7).

2. **Asymptotic Sampling Zeros** (ASZ) model: This model is similar to the SDR model (16), but we include the asymptotic sampling zeros defined by the Euler-Fröbenius polynomial, i.e.,

$$G_d^{ASZ}(z) = \frac{B_r(z)}{r!}G_d^{SDR}(z) \quad (18)$$

   The scaling factor $1/r!$ ensures $G_d^{ASZ}(1) = G(0)$.

   When r an even number, $B_r(z)$ has a root at $z = -1$. This makes the relative error corresponding to the ASZ model to grow to infinity as we approach the Nyquist frequency $\frac{\pi}{\Delta}$ (see Section 4). We thus also introduce a **Corrected Sampling Zeros** (CSZ) model that includes a refined approximation of the asymptotic sampling zero at $z = -1$ when r is an even number. We do this in order to keep the associated relative error bounded. The model is given by

$$G_d^{CSZ}(z) = \frac{K(z)}{K(1)}G_d^{ASZ}(z) \quad (19)$$

   where

$$K(z) = \frac{(z+1+c_\Delta)}{(z+1)} \quad (20)$$

   When r is an odd number, then $c_\Delta = 0$ and, as a consequence $G_d^{CSZ}(z) = G_d^{ASZ}(z)$. When r is an even number, then c_Δ is chosen such that an approximation of the order of Δ of the sampling zero around $z = -1$ is obtained [7], i.e.,

$$c_\Delta = \frac{\Delta}{r+1}\left\{\sum_{i=1}^{n} p_i - \sum_{k=1}^{m}\sigma_k\right\} \quad (21)$$

3. **Different-order Taylor Expansion** (DTE) model: This model was proposed in [22] for nonlinear systems expressed in the, so called, *normal form* [14] based on the idea that, for a system having relative degree r, one needs to differentiate the output r times in order to make the system input to appear explicitly. A state-space representation of a linear system in normal form is given by [14]

$$\begin{bmatrix} \dot{x}_1 \\ \vdots \\ \dot{x}_{r-1} \\ \dot{x}_r \\ \dot{\eta} \end{bmatrix} = \begin{bmatrix} x_2 \\ \vdots \\ x_r \\ Q_{11}\xi + Q_{12}\eta + u \\ Q_{21}\xi + Q_{22}\eta \end{bmatrix} \quad (22)$$

   where $\xi = [x_1, \ldots, x_r]^T$, $\eta = [x_{r+1}, \ldots, x_n]^T$, and the system output is $y = x_1$. Explicit expressions for Q_{ij} above are given in (50)-(53). An approximate sampled-data model is then obtained performing a Taylor series expansion of each state up to an order such that the input explicitly appears. This leads to the model

$$\begin{bmatrix} q\,x_1 \\ \vdots \\ q\,x_{r-1} \\ q\,x_r \\ q\,\eta \end{bmatrix} = \begin{bmatrix} x_1 + \Delta x_2 + \ldots + \frac{\Delta^r}{r!}(Q_{11}\xi + Q_{12}\eta + u) \\ \vdots \\ x_{r-1} + \Delta x_r + \frac{\Delta^2}{2}(Q_{11}\xi + Q_{12}\eta + u) \\ x_r + \Delta(Q_{11}\xi + Q_{12}\eta + u) \\ \eta_k + \Delta(Q_{21}\xi + Q_{22}\eta) \end{bmatrix} \tag{23}$$

where q is the forward shift operator, and the output of the sampled model is $y = x_1$. Thus, an associated transfer function $G_d^{DTE}(z)$ can be obtained from (23).

A consequence of Lemma 2 (below) for systems with relative degree r an even number, is that we have to introduce a **Corrected Different-order Taylor Expansion** (CTE) model in order to keep the associated relative error bounded near the Nyquist frequency (as we modified ASZ models to obtain CSZ models):

$$G_d^{CTE} = \frac{K(z)}{K(1)} G_d^{DTE}(z) \tag{24}$$

where $K(z)$ is defined in (20)-(21).

[9] considered the SDR, ASZ, and CSZ models and their associated maximum relative error. In this paper we include in our analysis the TDR model, based on the Tustin approximation of derivatives, and the two other models (DTE and CTE) that arise applying the sampling strategy proposed in [22]. In particular, the DTE model satisfies the following property:

Lemma 2. *Consider the approximate sampled-data model (23), where the output is $y = x_1$. Then, the zeros of the associated discrete time transfer function $G_d^{DTE}(z)$ are given by*

1. *An Euler approximation of the* intrinsic *zeros of the system, i.e., they appear at $z = 1 + \Delta\,\sigma_k$.*
2. *The asymptotic sampling zeros corresponding to a system of relative degree r, i.e., the roots of $B_r(z)$.*

Thus, the associated transfer function has the form

$$G_d^{DTE}(z) = \frac{B_r(z) F(\frac{z-1}{\Delta})}{r! \tilde{E}(z)} \tag{25}$$

Proof. It follows directly from [22, Theorem 2], where it is shown that the zero dynamics of the approximate sampled model are given by *(i)* the intrinsic zero dynamics discretized using Euler approximation, and *(ii)* the sampling zero dynamics, whose eigenvalues are equal to the asymptotic sampling zeros described by the Euler-Fröbenius polynomials. For linear systems, the eigenvalues of the zero dynamics correspond to the zeros of the transfer function [14]. □

The mapping of the continuous-time poles to the roots of $\tilde{E}(z)$ of the DTE model (25) is not straightforward to obtain (see Appendix A). This is in contrast to the exact sampled-data model (5), where the mapping of the poles is easily obtained, i.e., they appear at $z = e^{p_i \Delta}$, but the mapping of the zeros is much more involved. In fact, the mapping of the intrinsic and sampling zeros is thoroughly discussed in [7].

4 Relative errors

In this section we consider the error associated with each of the previous models when compared to the exact sampled-data model (4). We define the following relative error measures in the frequency domain:

$$R_1^i(\omega) = \left| \frac{G_d^{ESD}(e^{j\omega\Delta}) - G_d^i(e^{j\omega\Delta})}{G_d^{ESD}(e^{j\omega\Delta})} \right| \tag{26}$$

$$R_2^i(\omega) = \left| \frac{G_d^{ESD}(e^{j\omega\Delta}) - G_d^i(e^{j\omega\Delta})}{G_d^i(e^{j\omega\Delta})} \right| \tag{27}$$

where the superscript $i \in \{$SDR, TDR, ASZ, CSZ, DTE, CTE$\}$. The relative error above are defined for frequencies up to the Nyquist frequency, i.e., in the range $[0, \frac{\pi}{\Delta}]$.

Theorem 3. *The relative error performance of the approximate sampled-data models DTE, CTE and TDR are as follows:*

Relative error	*r: odd*	*r: even*
$\|R_1^{SDR}(\omega)\|_\infty$	$\mathcal{O}(1)$	$\mathcal{O}(\frac{1}{\Delta})$
$\|R_1^{TDR}(\omega)\|_\infty$	$\mathcal{O}(1)$	$\mathcal{O}(1)$
$\|R_1^{ASZ}(\omega)\|_\infty$	$\mathcal{O}(\Delta)$	$\mathcal{O}(1)$
$\|R_1^{CSZ}(\omega)\|_\infty$	$\mathcal{O}(\Delta)$	$\mathcal{O}(\Delta)$
$\|R_1^{DTE}(\omega)\|_\infty$	$\mathcal{O}(\Delta)$	$\mathcal{O}(1)$
$\|R_1^{CTE}(\omega)\|_\infty$	$\mathcal{O}(\Delta)$	$\mathcal{O}(\Delta)$

Relative error	*r: odd*	*r: even*
$\|R_2^{SDR}(\omega)\|_\infty$	$\mathcal{O}(1)$	$\mathcal{O}(1)$
$\|R_2^{TDR}(\omega)\|_\infty$	∞	∞
$\|R_2^{ASZ}(\omega)\|_\infty$	$\mathcal{O}(\Delta)$	∞
$\|R_2^{CSZ}(\omega)\|_\infty$	$\mathcal{O}(\Delta)$	$\mathcal{O}(\Delta)$
$\|R_2^{DTE}(\omega)\|_\infty$	$\mathcal{O}(\Delta)$	∞
$\|R_2^{CTE}(\omega)\|_\infty$	$\mathcal{O}(\Delta)$	$\mathcal{O}(\Delta)$

where $\|R(\omega)\|_\infty = \sup_{\omega\in[0,\frac{\pi}{\Delta}]} |R(\omega)|$

Proof. See Appendix A. □

Theorem 3 presents the maximum magnitude of the error as a function of the sampling period. However, no insights are given into the accuracy of the approximate models at different frequencies. The following section provides more details on the behavior of the relative errors for low and high frequencies.

5 Bandwidth of accuracy

In this section we present the main result of the paper: we characterize the bandwidth where each approximate sampled-data model provides higher accuracy.

Theorem 4. *Assume that $G(s)$ has relative degree $r > 1$, and has no pure imaginary poles or zeros. Then,*

1. *For* low *frequencies, SDR models are more accurate than ASZ models, i.e., when $\omega \to 0$,*

$$R_k^{SDR}(\omega) \leq R_k^{ASZ}(\omega) \tag{28}$$

where $k \in \{1, 2\}$.

2. *The frequencies at which SDR and ASZ models have approximately the same relative error are given by the solutions of the following equation*

$$\sum_{i=1}^{n} \frac{\omega^2}{\omega^2 + |p_i|^2} - \sum_{k=1}^{m} \frac{\omega^2}{\omega^2 + |\sigma_k|^2} = \frac{r+1}{2} \tag{29}$$

The solutions ω_ℓ of (29) *satisfy*

$$\check{p}\sqrt{\frac{r+1}{2n}} \leq \omega_\ell \leq \sqrt{\frac{(n+m+1)\widehat{p}^2 + \check{\sigma}^2}{r-1}} \tag{30}$$

where $\check{p}$, $\widehat{p}$, $\check{\sigma}$ and $\widehat{\sigma}$ denote the minimum and maximum magnitude of the system poles, and the minimum and maximum magnitude of the system zeros, respectively.

Proof. See Appendix B. □

The previous theorem can be extended to compare SDR and CSZ models, obtaining the same bounds that appear in (30). Moreover, the assumptions in Theorem 4 can be relaxed: If the relative degree of $G(s)$ is $r = 1$ then both approximate models, SDR and ASZ, are the same. On the other hand, if the continuous-time system includes pure imaginary poles or zeros, the relative error for both models, SDR and ASZ, go to zero or infinity at those frequencies, respectively (see Example 7).

Equation (29) can be numerically solved for any given system, however, the bounds for the roots established in (30) are, from our point of view, more insightful. Indeed, the bandwidth (30) at which the SDR and ASZ models have the same relative error depends only on the poles and zeros of the system, but is independent of the sampling period. This result provides a clear guideline to which approximate models are better to use: If one will use an approximate model up to the continuous-time system bandwidth, then SDR models may provide enough accuracy. However, if one requires a model more accurate for higher frequencies (and, in particular, near the Nyquist frequency), then the sampled model *has to incorporate sampling zeros*, as can be seen from the maximum relative errors in Theorem 3.

An interesting question at this point is how one can obtain a model as accurate as SDR models for low frequencies, but, at the same time, as accurate as ASZ (or CSZ) models for frequencies close to the Nyquist frequency $\frac{\pi}{\Delta}$. In fact, the next result shows that CTE models provide such desired behavior.

Theorem 5. *For a sampling period sufficiently small, the relative error associated with CTE models behaves as the relative error corresponding to SDR models for low frequencies and as the relative error corresponding to CSZ models near the Nyquist frequency, i.e.,*

$$R_k^{CTE}(\omega) \xrightarrow{\omega\to 0} R_k^{SDR}(\omega) \tag{31}$$

$$R_k^{CTE}(\omega) \xrightarrow{\omega\to \frac{\pi}{\Delta}} R_k^{CSZ}(\omega) \tag{32}$$

where $k \in \{1, 2\}$.

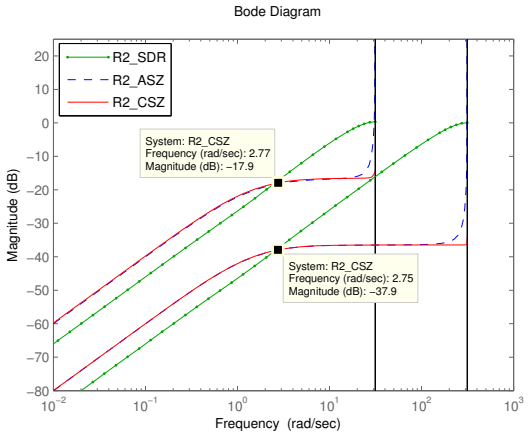

Figure 1: Relative errors $R_2^{SDR}(\omega)$, $R_2^{ASZ}(\omega)$ and $R_2^{CSZ}(\omega)$ for two different sampling periods $\Delta \in \{0.1, 0.01\}$ (Example 6).

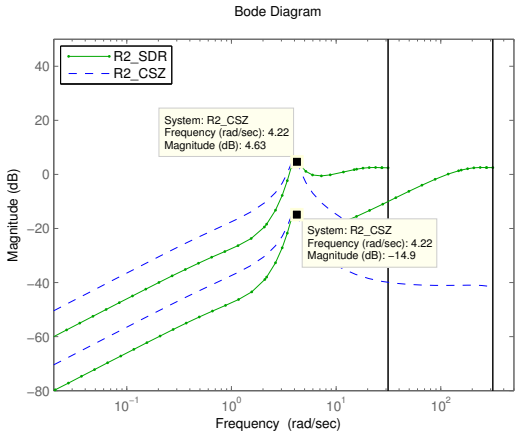

Figure 2: Relative errors $R_2^{SDR}(\omega)$ and $R_2^{CSZ}(\omega)$ for different sampling periods $\Delta \in \{0.1, 0.01\}$ (Example 7).

Proof. See Appendix C. □

6 Examples

In this section we present examples to illustrate the bounds presented in Theorem 4. Additionally, we analyze the accuracy of DTE and CTE models.

Example 6. *Consider* $G(s) = \frac{2}{(s+1)(s+2)}$. *The ESD, SDR, ASZ and CSZ models are as follow:*

$$G_d^{ESD}(z) = \frac{b_1(\Delta)z + b_0(\Delta)}{(z - e^{-\Delta})(z - e^{-2\Delta})} \tag{33}$$

$$G_d^{SDR}(z) = \frac{2}{(\frac{z-1}{\Delta} + 1)(\frac{z-1}{\Delta} + 2)} \tag{34}$$

$$G_d^{ASZ}(z) = \frac{(z+1)}{(\frac{z-1}{\Delta} + 1)(\frac{z-1}{\Delta} + 2)} \tag{35}$$

$$G_d^{CSZ}(z) = \frac{2(z+1-\Delta)}{(\frac{z-1}{\Delta} + 1)(\frac{z-1}{\Delta} + 2)(2-\Delta)} \tag{36}$$

The relative errors $R_2^{SDR}(\omega)$, $R_2^{ASZ}(\omega)$ *and* $R_2^{CSZ}(\omega)$ *of the approximate models are shown in Figure 1 for two different sampling periods,* $\Delta = 0.1$ *and* $\Delta = 0.01$. *The bounds predicted in Theorem 4 are given by* $0.8165 \leq \omega_\ell \leq 3.4641$. *Figure 1 shows that the frequency where relative errors intersect is within the band given in (6).*

Example 7. *We now consider a more complex system which includes a slightly damped resonant mode*

$$G(s) = \frac{p_1\omega_n^2}{(s+p_1)(s^2+2\xi\omega_n s+\omega_n^2)} \tag{37}$$

where $p_1 = 1$, $\xi = 0.1$, $\omega_n = 4$. *We obtain the SDR and CSZ models as in the previous example. In this case the asymptotic sampling zeros are the roots of* $B_3(z) = z^2 + 4z + 1$. *Note that for this system* $G_d^{ASZ}(z) = G_d^{CSZ}(z)$.

The relative errors $R_2^{SDR}(\omega)$ *and* $R_2^{CSZ}(\omega)$ *are shown in Figure 2, where we see that they intersect at* $\omega_\ell = 4.22$. *Note that this frequency is very close to the resonant mode of the system at* $\omega_n = 4$ *and within the band predicted by Theorem 4, i.e.,* $0.8165 \leq \omega_\ell \leq 5.6569$.

Example 8. *We consider again the continuous-time system in Example 7 and we compare the associated SDR and CSZ models with CTE models. In this case,* $G_d^{CSZ}(z) = G_d^{ASZ}(z)$ *and* $G_d^{DTE}(z) = G_d^{CTE}(z)$. *Figure 3 shows that CTE models provide the same relative error than SDR models for low frequencies. For higher frequencies, CTE models provide higher accuracy than SDR models, because they include the asymptotic sampling zeros. Moreover, we see that CTE models provides the highest accuracy for low and high frequencies, and it is only slightly outperformed by CSZ models in a band around* $\omega = 1$.

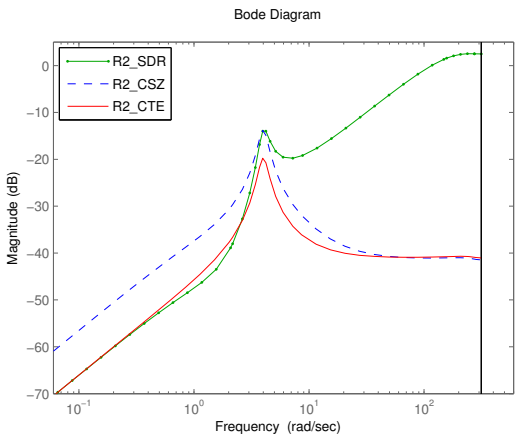

Figure 3: Relative errors $R_2^{SDR}(\omega)$, $R_2^{CSZ}(\omega)$ and $R_2^{CTE}(\omega)$, for a sampling period $\Delta = 0.01$ (Example 8).

7 Conclusion

In this paper we have characterized the accuracy of different approximate sampled-data models for linear systems in terms of frequency-domain relative error. We have shown that a simple derivative replacement model using Euler approximation provides a smaller relative error within the continuous-time system bandwidth. However, if one is required to have a more accurate model for higher frequencies (in particular, near the Nyquist frequency), then sampling zeros must be included in the model. Additionally, the results show that a particular model obtained by different-order Taylor expansion of the state equations provides an accurate description *for all frequencies.*

The insights provided by the relative error analysis presented in this paper can be taken into account for the case of approximate sampled data models for nonlinear systems. For these systems, even though relative errors in the frequency domain cannot be analyzed, approximate sampled models can be readily obtained using Euler, Tustin, or the proposed different-order Taylor expansion. The results presented here suggest that the latter kind of model is the best option. This complements the results in [22] where the accuracy was characterized in terms of time domain truncation errors.

A Proof of theorem 3

The $\mathcal{H}_\infty$-norm of $R_1^i(\omega)$ and $R_2^i(\omega)$ for SDR, ASZ, and CSZ models was characterized in [9]. Thus, the proof only considers the $\mathcal{H}_\infty$-norm analysis for TDR, DTE, and CTE models.

A key observation is that, for any fixed frequency $G_d^i(e^{j\omega\Delta}) \xrightarrow{\Delta\to 0} G(j\omega)$ This implies that, for any fixed ω, the relative errors (26) and (27) go to zero. Thus, the analysis is restricted to the behavior of the relative error at the Nyquist frequency $\omega_N = \frac{\pi}{\Delta} \Leftrightarrow z = -1$. Note that this frequency go to ∞ as the sampling period Δ goes to 0.

Let $G(s)$ be the linear system in (1) represented as

$$G(s) = \frac{s^m + b_{m-1}s^{m-1} + \cdots + b_1 s + b_0}{s^n + a_{n-1}s^{n-1} + \cdots + a_1 s + a_0} \tag{38}$$

where $b_{m-1} = -\sum_{k=1}^{m}\sigma_k$ and $a_{n-1} = -\sum_{i=1}^{n} p_i$. The transfer function (38) can be expanded as

$$G(s) = \tfrac{1}{s^r} + \Theta\tfrac{1}{s^{r+1}} + \mathcal{O}(s^{-r-2}) \tag{39}$$

$$\text{where} \qquad \Theta = b_{m-1} - a_{n-1} = \sum p_i - \sum \sigma_k \tag{40}$$

The ESD model for an r-th order integrator is given by the right hand side of (7) [3]. Thus, an expansion of the sampled model corresponding to (39) is given by

$$G_d^{ESD}(z) = \frac{\Delta^r B_r(z)}{r!(z-1)^r} + \Theta\frac{\Delta^{r+1}B_{r+1}(z)}{(r+1)!(z-1)^{r+1}} + \mathcal{O}(\Delta^{r+2}) \tag{41}$$

Moreover, $G(s)$ can be expressed in state-space form

$$\dot{x} = Ax + Bu \tag{42}$$

$$y = Cx \tag{43}$$

where

$$A = \left(\begin{array}{c|c} 0_{n-1\times 1} & I_{n-1} \\ \hline -a_0 & \dots\ -a_{n-1} \end{array}\right),\ B = \begin{pmatrix} 0_{n-1\times 1} \\ \hline 1 \end{pmatrix} \tag{44}$$

$$C = \begin{pmatrix} b_o & b_1 & \cdots & b_{m-1} & 1 & 0\cdots & 0 \end{pmatrix} \tag{45}$$

There exists a transformation $\begin{pmatrix}\xi\\ \eta\end{pmatrix} = \Phi x$ such that (42)-(45) is rewritten in the normal form [14]

$$\dot{\xi} = A_r\xi + B_r C A^r \Phi^{-1}\begin{pmatrix}\xi\\ \eta\end{pmatrix} + B_r u \tag{46}$$

$$\dot{\eta} = Q_{21}\xi + Q_{22}\eta \tag{47}$$

where

$$A_r = \left(\begin{array}{c|c} 0_{r-1\times 1} & I_{r-1} \\ \hline 0 & 0_{1\times r-1} \end{array}\right) \in \mathbb{R}^{r\times r}, \tag{48}$$

$$B_r = \begin{pmatrix} 0_{r-1\times 1} \\ \hline 1 \end{pmatrix} \in \mathbb{R}^{r} \tag{49}$$

$$Q_{21} = \left(\begin{array}{c|c} 0_{1\times r-1} & 0_{m-1\times r-1} \\ \hline 1 & 0_{r-1\times 1} \end{array}\right) \in \mathbb{R}^{m\times r} \tag{50}$$

$$Q_{22} = \left(\begin{array}{c|ccc} 0_{m-1\times 1} & & I_{m-1} & \\ \hline -b_0 & -b_1 & \cdots & -b_{m-1} \end{array}\right) \in \mathbb{R}^{m\times m} \tag{51}$$

and

$$\Phi = \left(\begin{array}{c} C \\ \vdots \\ CA^{r-1} \\ \hline I_m \;\vert\; \vec{0}_{m\times r} \end{array}\right) \tag{52}$$

Note that, comparing (46)-(51) with (22)

$$Q_{11}\xi + Q_{12}\eta + u = CA^r\Phi^{-1}\tbinom{\xi}{\eta} + u \tag{53}$$

Then the DTE model (23) is given by

$$q\,\xi = A_r^q\xi + B_r^q[CA^r\Phi^{-1}\tbinom{\xi}{\eta} + u] \tag{54}$$

$$q\,\eta = \Delta Q_{12}\xi + (I_m + \Delta Q_{22})\eta \tag{55}$$

where

$$A_r^q = e^{A_r\Delta} = \begin{pmatrix} 1 & \Delta & \cdots & \frac{\Delta^{r-1}}{(r-1)!} \\ 0 & & \ddots & \vdots \\ \vdots & \ddots & & \Delta \\ 0 & \cdots & 0 & 1 \end{pmatrix} \tag{56}$$

$$B_r^q = \int_0^\Delta e^{A_r\nu}B_r d\nu = \begin{pmatrix} \frac{\Delta^r}{r!} & \cdots & \Delta \end{pmatrix}^T \tag{57}$$

Equations (54) and (55) can be rewritten as

$$\tfrac{q-1}{\Delta}\;\xi = A_r^\delta\xi + B_r^\delta[CA^r\Phi^{-1}\tbinom{\xi}{\eta} + u] \tag{58}$$

$$\tfrac{q-1}{\Delta}\;\eta = Q_{21}\xi + Q_{22}\eta \tag{59}$$

where

$$A_r^\delta = \frac{A_r^q - I}{\Delta} = A_r + \mathcal{O}(\Delta) = \begin{pmatrix} 0 & 1 & \cdots & \frac{\Delta^{r-2}}{(r-1)!} \\ \vdots & \ddots & \ddots & \vdots \\ \vdots & \ddots & \ddots & 1 \\ 0 & \cdots & \cdots & 0 \end{pmatrix} \tag{60}$$

$$B_r^\delta = \frac{B_r^q}{\Delta} = B_r + \mathcal{O}(\Delta) = \begin{pmatrix} \frac{\Delta^{r-1}}{r!} & \cdots & 1 \end{pmatrix}^T \tag{61}$$

Then, the denominator of the transfer function (25) associated with the DTE model, is given by

$$\tilde{E}(z) = \det\left(\tfrac{z-1}{\Delta} - A_d\right) \tag{62}$$

where, from (58)-(59),

$$A_d = \left(\begin{array}{c|c} A_r^\delta & 0_{r\times m} \\ \hline 0_{m\times r} & 0_{m\times m} \end{array}\right) + \left(\begin{array}{c|c} B_r^\delta CA^r\Phi^{-1} & \\ \hline Q_{21} & Q_{22} \end{array}\right) \tag{63}$$

The characteristic polynomial (62) can be expanded as [5]:

$$\tilde{E}(z) = \tfrac{1}{\Delta^n}\{(z-1)^n - \mathrm{tr}(A_d)(z-1)^{n-1}\Delta + \mathcal{O}(\Delta^2)\} \tag{64}$$

Note that, from (46)-(47) ,

$$\Phi A\Phi^{-1} = \left(\begin{array}{c|c} A_r & 0_{r\times m} \\ \hline 0_{m\times r} & 0_{m\times m} \end{array}\right) + \left(\begin{array}{c|c} B_r CA^r\Phi^{-1} & \\ \hline Q_{21} & Q_{22} \end{array}\right) \tag{65}$$

From (45), (60), (61) and (63), we obtain

$$A_d = \Phi A\Phi^{-1} + \mathcal{O}(\Delta) \tag{66}$$

$$\Rightarrow \mathrm{tr}(A_d) = -\,a_{n-1} + \mathcal{O}(\Delta) \tag{67}$$

Then

$$\tilde{E}(z) = \left(\tfrac{z-1}{\Delta}\right)^n\left(1 + \tfrac{a_{n-1}\Delta}{z-1} + \mathcal{O}(\Delta)\right) \tag{68}$$

The numerator of (25) can be expressed as

$$\tilde{F}(z) = \tfrac{B_r(r)(z-1)^m}{r!\Delta^m}\left(1 + \tfrac{b_{m-1}\Delta}{z-1} + \mathcal{O}(\Delta^2)\right) \tag{69}$$

Equation (68) and (69) yields the following expansion

$$G_d^{DTE}(z) = \frac{\Delta^r B_r(z)}{r!(z-1)^r}\left\{\frac{1 + b_{m-1}\frac{\Delta}{z-1} + \mathcal{O}(\Delta^2)}{1 + a_{n-1}\frac{\Delta}{z-1} + \mathcal{O}(\Delta^2)}\right\} \tag{70}$$

$$= \tfrac{\Delta^r B_r(z)}{r!(z-1)^r} + \Theta\tfrac{\Delta^{r+1}B_r(z)}{r!(z-1)^{r+1}} + \mathcal{O}(\Delta^{r+2}) \tag{71}$$

From (41) and (71), the absolute error between DTE and ESD models is given by

$$G_d^{ESD} - G_d^{DTE} = \Theta\tfrac{\Delta^{r+1}\{B_{r+1} - (r+1)B_r\}}{(r+1)!(z-1)^{r+1}} + \mathcal{O}(\Delta^{r+2}) \tag{72}$$

Then

$$\tfrac{G_d^{ESD} - G_d^{DTE}}{G_d^{ESD}} = \tfrac{\Delta\Theta(B_{r+1} - (r+1)B_r)}{(r-1)(z-1)B_r + \Delta\Theta B_{r+1}} + \mathcal{O}(\Delta^2) \tag{73}$$

$$\tfrac{G_d^{ESD} - G_d^{DTE}}{G_d^{DTE}} = \tfrac{\Delta\Theta(B_{r+1} - (r+1)B_r)}{(r+1)((z-1)B_r + \Delta\Theta B_r)} + \mathcal{O}(\Delta^2) \tag{74}$$

where $B_r(z) = B_r$.

Then, replacing $\omega = \frac{\pi}{\Delta}$ ($z = -1$) in the relative errors (26) and (27), gives the result for DTE models:

$$R_1^{DTE}(\tfrac{\pi}{\Delta}) = \begin{cases} \mathcal{O}(\Delta) & r: \text{ odd} \\ \mathcal{O}(1) & r: \text{ even} \end{cases} \quad (75)$$

$$R_2^{DTE}(\tfrac{\pi}{\Delta}) = \begin{cases} \mathcal{O}(\Delta) & r: \text{ odd} \\ \infty & r: \text{ even} \end{cases} \quad (76)$$

For the case of the CTE models, we proceed similarly. When r is an odd number, then $G_d^{CTE}(z) = G_d^{DTE}(z)$ and the previous analysis gives the result. When r is an even number, then CTE models can be expressed as

$$\begin{aligned} G_d^{CTE}(z) &= \tfrac{z+1+c_\Delta}{(z+1)(1+\frac{c_\Delta}{2})} G_d^{DTE}(z) \\ &= (1+\tfrac{c_\Delta}{z+1})(1-\tfrac{1}{2}c_\Delta + \mathcal{O}(\Delta^2)) G_d^{DTE}(z) \\ &= (1-\tfrac{c_\Delta}{2}\tfrac{(z-1)}{(z+1)} + \mathcal{O}(\Delta^2)) G_d^{DTE}(z) \end{aligned} \quad (77)$$

Then, using (71) and noting that $c_\Delta = \frac{\Delta\Theta}{r+1}$, we obtain

$$\begin{aligned} G_d^{CTE}(z) = \tfrac{\Delta^r B_r(z)}{r!(z-1)^r} + \Theta\tfrac{\Delta^{r+1} B_r(z)}{r!(z-1)^{r+1}} + \\ - \Theta\tfrac{\Delta^{r+1} B_r(z)}{2(r+1)!(z+1)(z-1)^{r-1}} + \mathcal{O}(\Delta^{r+2}) \end{aligned} \quad (78)$$

Then taking the limit as $z \to -1$ and using *L'Hopital's rule* for the third term on the right hand side, we obtain

$$G_d^{CTE}(-1) = \Theta\tfrac{\Delta^{r+1} B_r'(-1)}{(r+1)!2^r} + \mathcal{O}(\Delta^{r+2}) \quad (79)$$

Evaluating the ESD model in $z = -1$, we obtain

$$G_d^{ESD}(-1) = \Theta\tfrac{\Delta^{r+1} B_{r+1}(-1)}{(r+1)!2^{r+1}} + \mathcal{O}(\Delta^{r+2}) \quad (80)$$

The absolute error between CTE and ESD models is given by

$$\begin{aligned} G_d^{ESD}(-1) - G_d^{CTE}(-1) = \\ - \Theta\tfrac{\Delta^{r+1}}{(r+1)!2^{r+1}}\Big\{B_r'(-1) + \tfrac{B_{r+1}(-1)}{2}\Big\} + \mathcal{O}(\Delta^{r+2}) \end{aligned} \quad (81)$$

From property (6) of the Euler-Fröbenius polynomials, the expression in brackets equal to zero. Thus,

$$G_d^{ESD}(-1) - G_d^{CTE}(-1) = \mathcal{O}(\Delta^{r+2}) \quad (82)$$

From (79), (80) and (82) we have that

$$\tfrac{G_d^{ESD}(-1) - G_d^{CTE}(-1)}{G_d^{ESD}(-1)} = \mathcal{O}(\Delta) \quad (83)$$

$$\tfrac{G_d^{ESD}(-1) - G_d^{CTE}(-1)}{G_d^{CTE}(-1)} = \mathcal{O}(\Delta) \quad (84)$$

Then, both relative errors (26) and (27) associated with CTE models (when r is an even number) are of the order of Δ at the Nyquist frequency, i.e.

$$R_k^{CTE}(\tfrac{\pi}{\Delta}) = \mathcal{O}(\Delta), \quad k \in \{1, 2\} \quad (r: \text{ even}) \quad (85)$$

For the case of the TDR model we proceed as follows:

$$G_d^{TDR}(z) = G\big(\tfrac{2}{\Delta}\tfrac{z-1}{z+1}\big) \quad (86)$$

From (39) we have that

$$G_d^{TDR}(z) = \Big(\tfrac{\Delta}{2}\tfrac{z+1}{z-1}\Big)^r + \Theta\Big(\tfrac{\Delta}{2}\tfrac{z+1}{z-1}\Big)^{r+1} + \mathcal{O}(\Delta^{r+2}) \quad (87)$$

From (41) and (87) we can approximate the absolute error between ESD and TDR models as

$$G_d^{ESD}(z) - G_d^{TDR}(z) = \Delta^r \tfrac{2^r B_r(z) - r!(z+1)^r}{2^r r!(z-1)^r} + \mathcal{O}(\Delta^{r+1}) \quad (88)$$

Then we have that

$$\tfrac{G_d^{ESD} - G_d^{TDR}}{G_d^{ESD}} = \Big|\tfrac{2^r B_r(z) - r!(z+1)^r}{2^r B_r(z)}\Big| + \mathcal{O}(\Delta) \quad (89)$$

$$\tfrac{G_d^{ESD} - G_d^{TDR}}{G_d^{TDR}} = \Big|\tfrac{2^r B_r(z) - r!(z+1)^r}{r!(z+1)^r}\Big| + \mathcal{O}(\Delta) \quad (90)$$

Evaluating the relative errors associated to TDR model at the Nyquist frequency, we obtain

$$R_1^{TDR}(\tfrac{\omega}{\Delta}) = \begin{cases} \mathcal{O}(1) & r: \text{ odd} \\ \mathcal{O}(1) & r: \text{even} \end{cases} \quad (91)$$

$$R_2^{TDR}(\tfrac{\omega}{\Delta}) = \begin{cases} \infty & r: \text{ odd} \\ \infty & r: \text{even} \end{cases} \quad (92)$$

This completes the proof.

B Proof of Theorem 4

We first obtain an approximation for ESD, SDR, and ASZ models. We consider the ESD model given in (3). This model can be equivalently expressed as in (6). When $\Delta \to 0$, the terms in the infinite sum (6) are negligible except for the term associated with $\ell = 0$. Thus, we use the following approximation

$$G_d^{ESD}(e^{s\Delta}) \approx (1 - e^{-s\Delta})\frac{G(s)}{s\Delta} = G(s)\left[1 - \tfrac{1}{2}s\Delta + \mathcal{O}(\Delta^2)\right] \quad (93)$$

Moreover, if we now examine the other terms in the infinite sum (6), and we replace $G(s)$ using (1), we have that

$$\begin{aligned}&\frac{(1-e^{-s\Delta})}{s\Delta+2\pi j\ell}\frac{\prod_{k=1}^{m}(s+2\pi j\ell/\Delta-\sigma_k)}{\prod_{i=1}^{n}(s+2\pi j\ell/\Delta-p_i)}\\&=\Delta^r\frac{1-e^{-s\Delta}}{s\Delta+2\pi j\ell}\frac{\prod_{k=1}^{m}(2\pi j\ell+\Delta(s-\sigma_k))}{\prod_{i=1}^{n}(2\pi j\ell+\Delta(s-p_i))}\\&=\mathcal{O}(\Delta^{r+1})\end{aligned}\tag{94}$$

Thus, all such terms are of the order of Δ^{r+1}, and do not modify the expansion in (93). Now, SDR models can be expressed as follows

$$G_d^{SDR}(e^{s\Delta})=G\left(\tfrac{e^{s\Delta}-1}{\Delta}\right)=G(s+\tfrac{s^2\Delta}{2}+\mathcal{O}(\Delta^2))\tag{95}$$

If we now replace $G(s)$ using (1), we obtain

$$\begin{aligned}G_d^{SDR}(e^{s\Delta})&=\frac{\prod_{k=1}^{m}(s+\frac{1}{2}s^2\Delta+\mathcal{O}(\Delta^2)-\sigma_k)}{\prod_{i=1}^{n}(s+\frac{1}{2}s^2\Delta+\mathcal{O}(\Delta^2)-p_i)}\\&=G(s)\left\{\frac{\prod_{k=1}^{m}(1+\frac{1}{2}\frac{s^2\Delta}{s-\sigma_k}+\mathcal{O}(\Delta^2))}{\prod_{i=1}^{n}(1+\frac{1}{2}\frac{s^2\Delta}{s-p_i}+\mathcal{O}(\Delta^2))}\right\}\end{aligned}\tag{96}$$

We then obtain a Taylor series expansion for the expression in curly brackets

$$G_d^{SDR}(e^{s\Delta})=G(s)\left\{1+\tfrac{1}{2}s\Delta\psi(s)+\mathcal{O}(\Delta^2)\right\}\tag{97}$$

$$\text{where}\quad\psi(s)=\sum_{k=1}^{m}\frac{s}{s-\sigma_k}-\sum_{i=1}^{n}\frac{s}{s-p_i}\tag{98}$$

We now obtain an approximation for the ASZ model. We see in (18) that this model is obtained including the asymptotic sampling zeros in the SDR model. A Taylor series expansion of $B_r(e^{j\omega\Delta})$, around $\Delta=0$ is given by

$$\begin{aligned}B_r(e^{s\Delta})&=B_r(1)+B_r'(1)s\Delta+\mathcal{O}(s^2\Delta^2)\\&=r!+\tfrac{r!(r-1)}{2}s\Delta+\mathcal{O}(s^2\Delta^2)\end{aligned}\tag{99}$$

where we have used the fact that $B_r(1)=r!$ and Lemma 1. Using (18), (97), and (99), we obtain

$$G_d^{ASZ}(e^{s\Delta})=G(s)\left\{1+\tfrac{1}{2}\left[\psi(s)+r-1\right]s\Delta+\mathcal{O}(\Delta^2)\right\}\tag{100}$$

From (97) and (100), the relative errors are expanded as

$$R_1^{SDR}(\omega)=\tfrac{1}{2}\left|\omega\Delta(1+\psi(j\omega))\right|+\mathcal{O}(\omega^2\Delta^2)\tag{101}$$

$$R_1^{ASZ}(\omega)=\tfrac{1}{2}\left|\omega\Delta(r+\psi(j\omega))\right|+\mathcal{O}(\omega^2\Delta^2)\tag{102}$$

$$R_2^{SDR}(\omega)=\tfrac{1}{2}\left|\omega\Delta(1+\psi(j\omega))\right|+\mathcal{O}(\omega^2\Delta^2)\tag{103}$$

$$R_2^{ASZ}(\omega)=\tfrac{1}{2}\left|\omega\Delta(r+\psi(j\omega))\right|+\mathcal{O}(\omega^2\Delta^2)\tag{104}$$

Then as $\omega\to 0$, the terms $\mathcal{O}(\omega^2\Delta^2)$ can be neglected for any sampling period Δ. Then, comparing (101) with (102), and (103) with (104) gives part 1) of the theorem

To show part 2) we consider the condition

$$R_k^{SDR}(\omega)=R_k^{ASZ}(\omega)\tag{105}$$

for $k\in\{1,2\}$. Using (101)-(104), it can be shown that (105) leads (for $k=1$ and for $k=2\}$) to

$$\left|\psi(j\omega)+r\right|=\left|\psi(j\omega)+1\right|+\mathcal{O}(\Delta)\tag{106}$$

If we neglect terms of the order of Δ in the last equation and we expand the magnitude in real an imaginary parts

$$\left[\mathfrak{Re}\Big\{\psi(j\omega)+r\Big\}\right]^2=\left[\mathfrak{Re}\Big\{\psi(j\omega)+1\Big\}\right]^2\tag{107}$$

Assuming $r>1$ and replacing $\psi(s)$ from (98) yields

$$\mathfrak{Re}\Big\{\psi(j\omega)\Big\}=\tag{108}$$

$$\begin{aligned}&=\sum_{k=1}^{m}\frac{\omega\left(\omega-\mathfrak{Im}\{\sigma_k\}\right)}{\omega^2+|\sigma_k|^2}-\sum_{i=1}^{n}\frac{\omega\left(\omega-\mathfrak{Im}\{p_i\}\right)}{\omega^2+|p_i|^2}\\&=-\frac{r+1}{2}\end{aligned}\tag{109}$$

Noting that complex poles and zeros appear in complex conjugate pairs, we obtain equation (29).

Now we find upper and lower bounds for the roots of

$$f(\omega)=\sum_{i=1}^{n}\frac{\omega^2}{\omega^2+|p_i|^2}-\sum_{k=1}^{m}\frac{\omega^2}{\omega^2+|\sigma_k|^2}-\frac{r+1}{2}\tag{110}$$

We find $\check{f}(\omega)$ and $\hat{f}(\omega)$ that minorize and majorize $f(\omega)$, respectively, i.e.

$$\check{f}(\omega)\le f(\omega)\le\hat{f}(\omega)\tag{111}$$

for all $\omega>0$, such that $\hat{f}(0)<0$ and $\lim_{\omega\to\infty}\check{f}(\omega)>0$, to ensure that the roots of $f(\omega)$ lie in the interval between the smallest positive root of $\check{f}(\omega)$ and the largest positive root of $\hat{f}(\omega)$. We choose

$$\check{f}(\omega)=n\tfrac{\omega^2}{\omega^2+\hat{p}^2}-m\tfrac{\omega^2}{\omega^2+\check{\sigma}^2}-\tfrac{r+1}{2}\tag{112}$$

The positive real root of this equation is $\omega=\omega_1$, where ω_1 is given in equation (112) at the top of the page. This is an upper bound for the roots of $f(\omega)$ in (110) . The frequency ω_1 can be bounded as

$$\omega_1\le\omega_2=\sqrt{\tfrac{(n+m+1)\hat{p}^2+\check{\sigma}^2}{r-1}}\tag{114}$$

$$\omega_1 = \sqrt{\frac{\hat{p}^2(1+n+m) - \check{\sigma}^2(m+n-1) + \sqrt{\check{\sigma}^4(n+m-1)^2 + 2(n^2-6nm+m^2-1)\check{\sigma}^2\hat{p}^2 + (1+n+m)^2\hat{p}^4}}{2(r-1)}} \tag{112}$$

where ω_2 its obtained adding the term

$$4\check{\sigma}^4(n+m) + 4(4nm+n+m+1)\check{\sigma}^2\hat{p}^2 \tag{115}$$

to the inner square root term in ω_1 in (112).

On the other hand, a majorizing function is given by

$$\hat{f}(\omega) = n\tfrac{\omega^2}{\check{p}^2} - \tfrac{r+1}{2} \tag{116}$$

Note that $\hat{f}(0) = -\frac{r+1}{2} < 0$, and thus, the lower bound for the roots of $f(\omega)$ is given by the only positive root of $\hat{f}(\omega)$, i.e.

$$\omega = \omega_3 = \check{p}\sqrt{\tfrac{r+1}{2n}} \tag{117}$$

Thus, the roots of $f(\omega)$ are bounded by (117) and (114).

C Proof of Theorem 5

To show that CTE relative errors behave as CSZ relatives errors, an approximation of ASZ model is first obtained. From (18) and (39) we have that

$$G_d^{ASZ}(z) = \frac{\Delta^r B_r(z)}{r!(z-1)^r} + \Theta\frac{\Delta^{r+1}B_r(z)}{r!(z-1)^{r+1}} + \mathcal{O}(\Delta^{r+2}) \tag{118}$$

From (118) and (19), and if r is an odd number, then

$$G_d^{CSZ} = G_d^{ASZ} = \frac{\Delta^r B_r(z)}{r!(z-1)^r} + \Theta\frac{\Delta^{r+1}B_r(z)}{r!(z-1)^{r+1}} + \mathcal{O}(\Delta^{r+2}) \tag{119}$$

When r is even number, the CSZ model takes the form

$$G_d^{CSZ}(z) = \tfrac{K(z)}{K(1)}G_d^{ASZ}(z) = \tfrac{2(z+1+c_\Delta)}{(z+1)(2+c_\Delta)}G_d^{ASZ}(z) \tag{120}$$

Expanding as in (77)

$$G_d^{CSZ}(z) = (1 - \tfrac{c_\Delta}{2}\tfrac{(z-1)}{(z+1)} + \mathcal{O}(\Delta^2))G_d^{ASZ}(z) \tag{121}$$

Replacing (118) into (121), and recalling that $c_\Delta = \frac{\Delta\Theta}{r+1}$, we obtain

$$\begin{aligned} G_d^{CSZ}(z) = {} & \tfrac{\Delta^r B_r(z)}{r!(z-1)^r} + \Theta\tfrac{\Delta^{r+1}B_r(z)}{r!(z-1)^{r+1}} + \\ & - \Theta\tfrac{\Delta^{r+1}B_r(z)}{2(r+1)!(z+1)(z-1)^{r-1}} + \mathcal{O}(\Delta^{r+2}) \end{aligned} \tag{122}$$

Comparing (78) and (122) it can be seen that CSZ and CTE models are equal up to an error of the order of Δ^{r+2}. From the relative error definitions (26)-(27), and after some manipulations, we obtain

$$|R_k^{CSZ} - R_k^{CTE}| = \mathcal{O}(\Delta^2) \qquad (k \in \{1,2\}) \tag{123}$$

Moreover, from Theorem 3, $R_k^i = \mathcal{O}(\Delta)$, for $i \in \{CSZ, CTE\}$ and $k = \{1,2\}$. Thus, in (123) and for a small Δ, near the Nyquist frequency $R_k^{CSZ} = R_k^{CTE}$. This corresponds to (32).

For low frequencies, CTE models can be expanded replacing $\frac{z-1}{\Delta} = s + \mathcal{O}(s^2\Delta)$ into (62). This yields

$$\begin{aligned} &\tilde{E}(e^{s\Delta}) = \det(sI - A_d + \mathcal{O}(s^2\Delta)) \\ &= \det(sI - A)\det(I + (A - A_d)(s-A)^{-1} + \mathcal{O}(s^2\Delta)) \\ &= E(s)\det(I - (A - A_d)(A^{-1} + sA^{-2} + \cdots) + \mathcal{O}(s^2\Delta)) \\ &= E(s)[\det(A_dA^{-1} - s(A - A_d)A^{-2}) + \mathcal{O}(s^2\Delta))] \\ &= E(s)[\det(A_dA^{-1}) \\ &\quad - \operatorname{tr}((A_dA^{-1})^A(A - A_d)A^{-2})s + \mathcal{O}(s^2\Delta)] \end{aligned} \tag{124}$$

where $(\cdot)^A$ denotes the adjugate matrix [5]. Simplifying the second term of the right side of (124)

$$\begin{aligned} &\operatorname{tr}((A_dA^{-1})^A(A - A_d)A^{-2}) \\ &= \det(A^{-1})\operatorname{tr}(A_d^A) - \det(A^{-1}A_d)\operatorname{tr}(A^{-1}) \end{aligned} \tag{125}$$

from (44) we have

$$A^{-1} = \begin{pmatrix} -\frac{a_1}{a_0} & \cdots & -\frac{a_{n-1}}{a_0} & -\frac{1}{a_0} \\ 1 & 0 & \cdots & 0 \\ & \ddots & \ddots & \vdots \\ & & 1 & 0 \end{pmatrix} \tag{126}$$

Then from the matrix (126) we see that

$$\det(A) = (-1)^n a_0, \quad \operatorname{tr}(A^{-1}) = -\tfrac{a_1}{a_0} \tag{127}$$

We now focus on obtaining the determinant of A_d. We denote

$$CA^r\Phi^{-1} = \begin{pmatrix} d_1 & d_2 & \cdots & d_{n-1} & d_n \end{pmatrix} \tag{128}$$

Thus,

$$\det(A_d) = \tag{129}$$

$$\left|\begin{array}{ccccc|ccc} \frac{\Delta^{r-1}}{r!}d_1 & \cdots & \frac{\Delta^{r-2}}{(r-1)!}+\frac{\Delta^{r-1}}{r!}d_r & \frac{\Delta^{r-1}}{r!}d_{r+1} & \cdots & \frac{\Delta^{r-1}}{r!}d_n \\ \vdots & \ddots & \vdots & \vdots & \ddots & \vdots \\ \frac{\Delta}{2}d_1 & \cdots & \frac{\Delta}{2}d_r+1 & d_{r+1} & \cdots & d_n \\ d_1 & \cdots & d_r & d_{r+1} & \cdots & d_n \\ \hline \multicolumn{2}{c}{Q_{21}} & & \multicolumn{3}{c}{Q_{22}} \end{array}\right| \tag{130}$$

Using the multi-linearity properties of determinants, it can be shown that

$$\det(A_d) = \left|\begin{array}{ccccc|ccc} 0 & 1 & \cdots & \frac{\Delta^{r-2}}{(r-1)!} & & 0 & \cdots & 0 \\ & & \ddots & \vdots & & \vdots & \ddots & \vdots \\ & & & 1 & & & & \\ d_1 & \cdots & & d_r & & d_{r+1} & \cdots & d_n \\ \hline \multicolumn{4}{c}{Q_{21}} & & \multicolumn{3}{c}{Q_{22}} \end{array}\right| \tag{131}$$

We then compute the determinant recursively from the first row down to the $(m-1)$-th row of Q_{22} (see equation (51)), i.e.,

$$\det(A_d) = (-1)^{n-r-1}\left|\begin{array}{cccc|c} 0 & 1 & \cdots & \frac{\Delta^{r-2}}{(r-1)!} & 0 \\ & & \ddots & \vdots & \vdots \\ & & & 1 & 0 \\ d_1 & \cdots & & d_r & d_{r+1} \\ \hline 1 & 0 & \cdots & 0 & -b_0 \end{array}\right| \tag{132}$$

We then compute the determinant recursively starting from the $(r-1)$-th to the first row, i.e.,

$$\begin{aligned} \det(A_d) &= (-1)^n \begin{vmatrix} d_1 & d_{r+1} \\ 1 & -b_0 \end{vmatrix} \\ &= (-1)^{n-1}(b_0 d_1 + d_{r+1}) \end{aligned} \tag{133}$$

To obtain d_1 and d_{r+1}, from (52), we have that

$$\Phi \vec{e}_1 = b_0 \vec{e}_1 + \vec{e}_{r+1} \tag{134}$$

Then, multiplying (134) by $CA^r\Phi^{-1}$, we obtain

$$CA^r\vec{e}_1 = b_0 CA^r\Phi^{-1}\vec{e}_1 + CA^r\Phi^{-1}\vec{e}_{r+1} \tag{135}$$

Notice that

$$CA^r = \begin{pmatrix} -a_0 \\ \vdots \\ -a_{n-r-1} \\ b_0 - a_{n-r} \\ \vdots \\ b_{m-1} - a_{n-1} \end{pmatrix}^T \tag{136}$$

Thus, using (128) and (136) into (135), we have

$$b_0 d_1 + d_{r+1} = -a_0 \tag{137}$$

Replacing into (133), it follows that

$$\det(A_d) = (-1)^n a_0 \tag{138}$$

The last equation will be used into (125), where the only term that we need is $\mathrm{tr}(A_d^A)$, which corresponds to the sum of the cofactors of A_d on the diagonal. We denote as c_i the cofactor corresponding to the i-th row and i-th column of A_d matrix. Then,

$$\mathrm{tr}(A_d^A) = \sum_{i=1}^{n} c_i \tag{139}$$

We compute the cofactors following a similar procedure as before when we obtained $\det(A_d)$. This yields, for $i = 1$,

$$\begin{aligned} c_1 &= (-1)^{n-r-1}\left|\begin{array}{cccc|c} 0 & 1 & \cdots & \frac{\Delta^{r-2}}{(r-1)!} & 0 \\ \vdots & & \ddots & \vdots & \vdots \\ & & & 1 & 0 \\ d_2 & \cdots & \cdots & d_r & d_{r+1} \\ \hline 0 & \cdots & \cdots & 0 & -b_0 \end{array}\right| \\ &= (-1)^{n-1}\begin{vmatrix} d_2 & d_{r+1} \\ 0 & -b_0 \end{vmatrix} \\ &= (-1)^n d_2 b_0 \end{aligned} \tag{140}$$

and, for $i \in \{2, \ldots, r\}$,

$$\begin{aligned} c_i &= (-1)^{n-r-1}\times \\ &\left|\begin{array}{ccc|c|ccc|c} 0 & \cdots & \frac{\Delta^{i-2}}{(i-1)!} & 0 & \frac{\Delta^i}{(i+1)!} & \cdots & \frac{\Delta^{r-2}}{(r-1)!} & 0 \\ & \ddots & \vdots & \vdots & \vdots & & & \vdots \\ & & 0 & 0 & \frac{\Delta}{2} & \cdots & \frac{\Delta^{r-i}}{(r-i+1)!} & \vdots \\ \hline 0 & \cdots & \cdots & 1 & 0 & \cdots & 0 & 0 \\ \hline & & & 0 & 0 & \cdots & \frac{\Delta^{r-i-2}}{(r-i-1)!} & \\ & & & \vdots & & \ddots & \vdots & \\ d_1 & \cdots & d_{i-1} & 0 & d_{i+1} & \cdots & d_r & \vdots \\ \hline 1 & 0 & \cdots & 0 & & \cdots & 0 & -b_0 \end{array}\right| \\ &= (-1)^{n-1}\frac{\Delta}{2}\begin{vmatrix} d_1 & d_{r+1} \\ 1 & -b_0 \end{vmatrix} \\ &= \tfrac{\Delta}{2}(-1)^{n-1}a_0 \quad i \in \{2, \ldots, r\} \end{aligned} \tag{141}$$

where the last equation follows from (137).

For $i = r+1$, the corresponding cofactor is given

by

$$c_{r+1} = (-1)^{n-r-1} \left| \begin{array}{cccc|c} 0 & 1 & \cdots & \frac{\Delta^{r-2}}{(r-1)!} & 0 \\ & & \ddots & \vdots & \vdots \\ & & & 1 & 0 \\ d_1 & \cdots & \cdots & d_r & d_{r+2} \\ \hline 1 & 0 & \cdots & 0 & -b_1 \end{array} \right|$$
$$= (-1)^{n-1} \begin{vmatrix} d_1 & d_{r+2} \\ 1 & -b_1 \end{vmatrix}$$
$$= (-1)^n (b_1 d_1 + d_{r+2}) \quad (142)$$

Finally, for $i \in \{r+2, \dots n\}$, we have that

$$c_i = \left| \begin{array}{c|ccc|c|ccccc} * & & & & 0 & & & & & \\ \hline & 0 & 1 & & & & & & & \\ & & \ddots & & 0 & & & & & \\ & & \ddots & & \vdots & & & & & \\ & & & 1 & 0 & & & & & \\ & 0 & \cdots & 0 & 0 & & & & & \\ \hline 0 & & \cdots & & 1 & 0 & & \cdots & & 0 \\ \hline & & & & & 0 & 1 & & & \\ & & & & \vdots & & \ddots & \ddots & & \\ & & & & & & & 0 & & 1 \\ * & -b_0 & \cdots & \cdots & 0 & \cdots & \cdots & & & -b_{m-1} \end{array} \right| \quad (143)$$

and we see that the $(i-1)$-th row is the zero row vector, therefore

$$c_i = 0, \quad i \in \{r+2, \dots, n\} \quad (144)$$

We now need to obtain d_2 and d_{r+2}. From (52), we see that

$$\Phi \vec{e}_2 = b_1 \vec{e}_1 + b_0 \vec{e}_2 + \vec{e}_{r+2} \quad (145)$$

Then, multipliying (145) by $CA^r\Phi^{-1}$, and using (136), we obtain

$$CA^r \vec{e}_2 = b_1 d_1 + b_0 d_2 + d_{r+2} = -a_1 \quad (146)$$

Therefore, from (140), (142) and (146) we have

$$c_1 + c_{r+1} = (-1)^{n-1} a_1 \quad (147)$$

From (126), (141), (144) and (147), we obtain

$$\det(A^{-1}) \mathrm{tr}(A_d^A) = -\tfrac{a_1}{a_0} - \tfrac{(r-1)\Delta}{2} \quad (148)$$

Thus,

$$\det(A^{-1}) \mathrm{tr}(A_d^A) - \det(A^{-1} A_d) \mathrm{tr}(A^{-1}) = -\tfrac{(r-1)\Delta}{2}$$

Finally, replacing into (124), we obtain

$$\tilde{E}(e^{s\Delta}) = E(s)\{1 + \tfrac{(r-1)\Delta}{2} s + \mathcal{O}(s^2\Delta)\} \quad (149)$$

From (99) and (149), for low frequencies the following expansion is obtained

$$G_d^{DTE}(e^{s\Delta}) = G(s) \left\{ \frac{1 + \frac{(r-1)}{2} s\Delta^2 + \mathcal{O}(s^2\Delta)}{1 + \frac{(r-1)}{2} s\Delta^2 + \mathcal{O}(s^2\Delta)} \right\}$$
$$= G(s)\{1 + \mathcal{O}(s^2\Delta)\} \quad (150)$$

Then, when the relative degree r is an odd number,

$$G_d^{CTE}(e^{s\Delta}) = G_d^{DTE}(e^{s\Delta}) = G(s)\{1 + \mathcal{O}(s^2\Delta)\} \quad (151)$$

On the other hand, when r is an even number, the correction term (20) has to be included, obtaining a similar expansion:

$$G_d^{CTE}(e^{s\Delta}) = \frac{K(e^{s\Delta})}{K(1)} G_d^{DTE}(e^{s\Delta})$$
$$= \frac{1 + \frac{c_\Delta}{e^{s\Delta}+1}}{1 + \frac{c_\Delta}{2}} G_d^{DTE}(e^{s\Delta})$$
$$= [1 + \mathcal{O}(s\Delta^2)] G_d^{DTE}(e^{s\Delta})$$
$$= G(s)\{1 + \mathcal{O}(s\Delta^2 + s^2\Delta)\} \quad (152)$$

Equations (93) and (151) (or (152)) yield

$$\tfrac{G_d^{ESD}(e^{s\Delta}) - G_d^{CTE}(e^{s\Delta})}{G_d^{ESD}(e^{s\Delta})} = \tfrac{\Delta}{2} s + \mathcal{O}(s^2\Delta + s\Delta^2) \quad (153)$$
$$\tfrac{G_d^{ESD}(e^{s\Delta}) - G_d^{CTE}(e^{s\Delta})}{G_d^{CTE}(e^{s\Delta})} = \tfrac{\Delta}{2} s + \mathcal{O}(s^2\Delta + s\Delta^2) \quad (154)$$

Thus, the relative errors (26)-(27) can be expanded as

$$R_k^{CTE}(\omega) = \tfrac{\Delta}{2}\omega + \mathcal{O}(\omega^2\Delta + \omega\Delta^2), \quad k \in \{1, 2\} \quad (155)$$

Note that $\psi(j\omega)$ in (98) is of the order of ω. Then, the expansion of the relative errors associated to SDR models ((101) and (103)) can be expressed as

$$R_k^{SDR}(\omega) = \tfrac{\Delta}{2}\omega + \mathcal{O}(\omega^2\Delta + \omega\Delta^2)), \; k \in \{1, 2\} \quad (156)$$

From (155) and (156) the error between the relative errors associated with CTE and CSZ models satisfy

$$R_k^{CTE}(\omega) - R_k^{CSZ}(\omega) = \mathcal{O}(\omega^2\Delta + \omega\Delta^2), \; k \in \{1, 2\} \quad (157)$$

For a sampling period sufficiently small, and for low frequencies, the terms of order $\omega^2 + \omega\Delta$ go to zero, and thus, the relative errors associated to CTE and CSZ models are approximately the same. This shows (31).

References

[1] J. C. Agüero, G. C. Goodwin, T. Söderström, and J. I. Yuz. Sampled data errors in variables systems. In *15th IFAC Symposium on System Identification - SYSID 2009*, Saint Malo, France, 5-8 July 2009.

[2] I. Arriagada and J. I. Yuz. On the relationship between splines, sampling zeros and numerical integration in sampled-data models for linear systems. In *American Control Conference, ACC 2008*, Seattle, USA, 2008.

[3] K. J. Åström, P. Hagander, and J. Sternby. Zeros of sampled systems. *Automatica*, 20(1):31–38, 1984.

[4] K. J. Åström and B. Wittenmark. *Computer Controlled Systems. Theory and Design*. Prentice Hall, Englewood Cliffs, N. J., 3rd edition, 1997.

[5] D. S. Bernstein. *Matrix Mathematics: Theory, Facts, and Formulas*. Princeton University Press, 2nd edition, 2009.

[6] M. J. Blachuta. On approximate pulse transfer functions. *IEEE Transactions on Automatic Control*, 44(11):2062–2067, 1999.

[7] M. J. Blachuta. On zeros of pulse transfer functions. *IEEE Transactions on Automatic Control*, 44(6):1229–1234, 1999.

[8] R. V. Churchill and J. W. Brown. *Complex Variables And Applications*. McGraw-hill, Englewood Cliffs, New Jersey, 8th edition, 2008.

[9] G. C. Goodwin, J. I. Yuz, and J. C. Agüero. Relative error issues in sampled-data models. In *17th IFAC World Congress*, Seoul, Korea, 2008.

[10] G. C. Goodwin, J. I. Yuz, J. C. Agüero, and M. Cea. Sampling and sampled-data models. In *2010 American Control Conference*, Baltimore, USA, 30 June - 2 July 2010.

[11] G. C. Goodwin, J. I. Yuz, and M. E. Salgado. Insights into the zero dynamics of sampled-data models for linear and nonlinear stochastic systems. In *European Control Conference - ECC'07*, Kos, Greece, 2-5 July 2007.

[12] T. Hagiwara, T. Yuasa, and M. Araki. Stability of the limiting zeros of sampled-data systems with zero- and first- order holds. *International Journal of Control*, 58(6), 1993.

[13] M. Ishitobi and M. Nishi. Zero dynamics of sampled-data models for nonlinear systems. In *American Control Conference, 2008*, May 2008.

[14] A. Isidori. *Nonlinear Control Systems*. Springer, 3rd edition, 1995.

[15] N. Kazantzis and C. Kravaris. System-theoretic properties of sampled-data representations of nonlinear systems obtained via Taylor-Lie series. *International Journal of Control*, 67(9):997–1020, 1997.

[16] S. Monaco and D. Normand-Cyrot. Zero dynamics of sampled nonlinear systems. *Systems and Control Letters*, 11:229–234, 1988.

[17] D. Nešić and A. R. Teel. A framework for stabilization of nonlinear sampled-data systems based on their approximate discrete-time models. *IEEE Transactions on Automatic Control*, 49(7):1103–1122, July 2004.

[18] C. Silva and J. I. Yuz. On sampled-data models for model predictive control. In *36th Annual Conference of the IEEE Industrial Electronics Society IECON 2010*, Phoenix, USA, 7-10 November 2010.

[19] B. Wahlberg. Limit results for sampled systems. *International Journal of Control*, 48(3):1267–1283, 1988.

[20] S. R. Weller, W. Moran, B. Ninness, and A. D. Pollington. Sampling zeros and the Euler-Fröbenius polynomials. *IEEE Transactions on Automatic Control*, 46(2):340–343, February 2001.

[21] J. I. Yuz and G. C. Goodwin. Generalised filters and stochastic sampling zeros. In *Joint CDC-ECC'05*, Seville, Spain, December 2005.

[22] J. I. Yuz and G. C. Goodwin. On sampled-data models for nonlinear systems. *IEEE Transactions on Automatic Control*, 50(10):1477–1489, October 2005.

[23] J. I. Yuz and G. C. Goodwin. Sampled-data models for stochastic nonlinear systems. In *14th IFAC Symposium on System Identification, SYSID 2006*, Newcastle, Australia, March 2006.

[24] J. I. Yuz, G. C. Goodwin, and H. Garnier. Generalised hold functions for fast sampling rates. In *43rd IEEE Conference on Decision and Control*, Nassau, Bahamas, December 2004.